Am J Transl Res 2019;11(7):4367-4381
www.ajtr.org /ISSN:1943-8141/AJTR0091440

Original Article

HEY2 acting as a co-repressor with smad3 and smad4 interferes with the response of TGF-beta in hepatocellular carcinoma

Jianqing Wang[1], Bo Zhu[1,2], Yuanyuan Zhang[2], Hexige Saiyin[2], Reziya Wumaier[1], Long Yu[2], Lichun Sun[3], Qianyi Xiao[1]

[1]Department of Preventive Medicine, Key Laboratory of Public Health Safety of The Ministry of Education, School of Public Health, Fudan University, 138 Yixueyuan Rd, Shanghai 200032, China; [2]State Key Laboratory of Genetic Engineering, Collaborative Innovation Center for Genetics and Development, School of Life Sciences, Fudan University, Shanghai, China; [3]Department of Medicine, School of Medicine, Tulane Health Sciences Center, New Orleans, LA 70112-2699, USA

Received January 17, 2019; Accepted June 3, 2019; Epub July 15, 2019; Published July 30, 2019

Abstract: The HEY2 (hairy and enhancer of split-related with YRPW motif 2) is reported to play potential roles in tumorigenesis. However, the underlying mechanism in tumorigenesis is remain elusive. The present study aims to investigate the molecular mechanism of biological function of HEY2 in hepatocellular carcinoma (HCC). Dysfunction of the transforming growth factor-beta (TGF-β) pathway plays a critical role in HCC pathogenesis. Here, we identified HEY2 as a suppressor for TGF-β biological response. We demonstrated that HEY2 protein in tumor cytoplasm was up-regulated in HCC. Further, HEY2 overexpression inhibited TGF-β-induced growth arrest of HCC cells and inhibited TGF-β-induced downregulation of c-Myc, both in mRNA and in protein levels. While knockdown of HEY2, by small interfering RNA, was shown to enhance the TGF-β-mediated biological response of HCC cells. Moreover, HEY2 could form complexes with Smad3 and Smad4 and repress Smad3/Smad4 transcriptional activity. In conclusion, our findings indicate a novel role of HEY2 in mediating the TGF-β/Smad signaling pathway in HCC tumorigenesis.

Keywords: HEY2, TGF-β, Smad, hepatocellular carcinoma (HCC), cell growth

Introduction

Hepatocellular carcinoma (HCC), the most frequently occurring primary liver cancer, ranks as the second leading cause of cancer-related death in men and the sixth in women [1]. The transforming growth factor-beta (TGF-β) signaling pathway plays a critical and dual role in the progression of HCC and many other types of cancer [2-5]. In the early phase of HCC progression, TGF-β protects homeostasis by functioning as a tumor suppressor, such as arresting cell cycle, inhibiting cell proliferation and inducing cell apoptosis [6-8]. Paradoxically, TGF-β also acts as a tumor promoter by stimulating cell migration and invasion through inducing epithelial-mesenchymal transition (EMT) in the late stages of tumor progression [9-12]. Dysfunctions of the TGF-β pathway and the switch of TGF-β responses towards malignancy play an important role in HCC pathogenesis.

TGF-β signals via activation of transmembrane hetero-oligomeric complexes of type I and type II serine/threonine kinase receptors, to intracellular mediators Samd2 and Samd3, which were called receptor-activated Smad (R-Smad) proteins. The cytoplasm phosphorylated R-Smads form complex with a common mediator Smad4 and then translocate to the nucleus, where this Smads complex regulates gene expression either directly or in association with coactivators and corepressors [13-15].

The c-Myc proto-oncogene is a critical downstream target of TGF-β/Smad pathway and its downregulation is a key event in the TGF-β program of growth inhibition [16, 17]. Amplification of c-Myc has been described in many human tumors [18]. Overexpression of c-Myc overcomes TGF-β-induced cell growth inhibition, and the loss of TGF-β-induced suppression of c-Myc correlates well with TGF-β resistance in breast

cancer [16], thyroid cancer [19], and ovarian cancer [20].

Hairy and enhancer of split-related with a YRPW motif protein 2 (HEY2), also known as HRT2, HESR2, HERP1 and CHF1, belongs to the HEY family of basic helix-loop-helix (bHLH) transcription factor [21, 22]. During embryogenesis, HEY2 is expressed in the ventricular myocardium, cardiac outflow tract and aortic arch arteries [23, 24]. HEY2 is the downstream target of Notch signaling and functions as transcriptional repressor to regulate gene transcription [25, 26]. The repressive influence of the HEY2 may result in part from an interaction with the other transcriptional factors to form corepressor complex [27, 28]. HEY2 exerts biological function on embryonic and cardiovascular development. Mouse lacking HEY2 leads to cardiomyopathy, cardiac defects, and ventricular septal defects with high postnatal lethality, whereas deletion of HEY1 has no apparent phenotypic defect [29-32]. The combined loss of HEY1 and HEY2 results in embryonic lethality with a global lack of vascular remodeling and massive hemorrhage [29]. Increasing evidence suggests that HEY2 is overexpressed and plays an important role in the development of various types of human cancers, including of osteosarcoma [33], prostate cancer [34], hepatocellular carcinoma [35], pancreatic ductal adenocarcinomas [36] and hemangioma [36]. Moreover, high expression of HEY2 correlates with poor survival in prostate cancer [34] and hepatocellular carcinoma [35]. Although the HEY2 is reported to play potential roles in tumorigenesis, the underlying mechanism remains poorly understood.

The present study demonstrates that HEY2 protein in tumor cytoplasm is up-regulated in HCC. HEY2 blocks TGF-β-induced growth inhibition of HCC cells through the inhibition of Smad3/Smad4 transcriptional activity. These results indicate that HEY2 may act as a potential modulator of TGF-β/smad signaling pathway in HCC tumorigenesis.

Materials and methods

Cell lines, cell culture and transient transfection

The human HCC cell lines Hep3B and HepG2, human embryonic kidney cell line 293T and the human cervical adenocarcinoma cell line HeLa were obtained from the American Type Culture Collection (ATCC). All these cell lines were cultured in DMEM medium containing 10% (vol/vol) fetal bovine serum at 37°C in a humidified incubator with 5% CO_2. Cells were transiently transfected using Lipo2000 (Invitrogen) according to the manufacturer's instructions.

Human tissue samples and tissue microarray

Primary HCC tissues and the corresponding non-tumorous liver tissues from surgical resection were obtained from HCC patients at Zhongshan Hospital (Shanghai, China). Ethical approval was obtained from the Research Ethics Committee of Zhongshan Hospital and Medical Ethics Committee of Fudan University. Written informed consent was obtained from each patient or patients' guardian.

The tissue microarray (TMA) was constructed by Shanghai Xinchao Biotechnology Co. Ltd (Xinchao Biotechnology Co, Shanghai, China). TMA sections with a thickness of 4 μm were dewaxed and pretreated in a microwave oven. Endogenous peroxide was blocked with 3% H_2O_2 in methanol for 10 min, followed by avidin-biotin blocking. Slides were incubated with human HEY2 antibody (NBP1-88629, Novus, 1:300) overnight at 4°C and incubated with biotinylated secondary antibodies, followed by treatment with peroxidase-labeled streptavidin for 10 min. The slides were washed thoroughly with PBS and the antibody reaction was visualized using a substrate solution containing diaminobenzidine (DAB). The sections were counter-stained with hematoxylin, dehydrated and mounted.

Quantification of HEY2 expression and statistical analysis

The immunostaining score of HEY2 in a tissue microarray was semiquantified by Quick-score (Q-score) based on intensity and heterogeneity of staining [37-39]. Briefly, the intensity of staining was scored as 0 (negative), 1 (weak), 2 (moderate), and 3 (strong), respectively. For the heterogeneity of staining, the positive rate was scored as 0 (0%), 1 (1-25%), 2 (26-50%), 3 (51-75%), and 4 points (76-100%), respectively. The Q-score was the sum of heterogeneity and intensity and ranged from 0 to 7. Each sample was scored blindly by two pathologists. Wil-

coxon matched paired test was used to determine the significance of HEY2 expression in HCC and adjacent non-cancerous tissues. We tested a cutoff value for the Q-score starting from a score of 3 to 5 and chose a score of 4 as the cutoff value to define high (Q-score >4) or low (Q-score ≤4) expression level of HEY2 in tumors. Chi-squared test was used to analyze the correlation between HEY2 expression anclinicopathological parameters. $P<0.05$ was considered to be statistically significant.

Stable cell lines for overexpression of HEY2

HEY2 cDNAs were amplified from the Marathon fetal liver cDNA library (Clontech) and subcloned into a mammalian expression vector pcDNA3.1Myc-His/B(-) (Invitrogen) containing neomycin resistance gene for establishment of stable cell lines, and into pCMV-Myc (Clontech). For stable transfection, at 24 hours after transfection with pcDNA3.1Myc-His/B(-)-HEY2, Hep-3B cells were passaged at 1:6 into new dishes and were selected with 400 μg/mL G418 (Invitrogen) for 14 days. Individual colonies expressing HEY2 were isolated and confirmed by western blot and maintained on the same selection medium. Control colonies stably transfected with pcDNA3.1Myc-His/B(-) were also generated in parallel.

Small interference RNA (siRNA)

SiRNA oligo for HEY2 were purchased from Genepharma (Shanghai, China). The siRNA oligo sequences for HEY2 is: 5'-CUCAGAUUAUGGCAAGAAAdTdT-3'. The sequence of negative control is: 5'-UUCUCCGAACGUGUCACGUdTdT-3'. The knockdown efficiency was determined by western blot.

Western blot

Protein samples from cells were separated by SDS-PAGE and then electro-transferred onto nitrocellulose membranes. After blocking with TBST buffer containing 5% skimmed milk, the membranes were incubated at 4°C overnight with primary antibodies against different proteins, followed by incubation with peroxidase-conjugated secondary antibody. Immunoreactivity was visualized by enhanced chemi-luminescence (Santa Cruz). The related antibodies include Myc (Sigma), HA (Sigma), Actin (Sigma), HEY2 (GTX87082, Genetex) for western bolt, HEY2 (NBP1-88629, Novus) for immunohistochemistry and western bolt, and c-Myc (Cell Signal).

Quantitative real-time PCR

Real-time PCR was performed using SYBR Green PCR master mix (TOYOBO) with the iCycler detection system (Bio-Rad). Blank controls with no cDNA templates were done to rule out contamination. Gene expression levels were normalized to the housekeeping gene β2-microglobulin (β2-MG). Primers of c-Myc, β2-MG, p15 and p21 are shown in Table S1.

MTS assay

Transfected cells were plated onto 96-well plates (Falcon) at a density of 1,000 cells per well and grown with or without 2 ng/ml TGF-β. During the culture period, cells were subjected to 3-(4,5-dimethyl-thiazol-2yl)-5-(3-carboxymethoxyphenyl)-2-(4-sulfophenyl)-2H-tetrazolium (MTS) assay (Promega) every two days. The Spectrophotometric absorbance of each well was measured at 490 nm after 3 hours incubation using a microtiter reader (Bio-Rad).

Colony formation assay

Colony formation assays were done with a high cell density as indicated in related figure legend, because long-term stimulation by TGF-β can cause cell cycle arrest and apoptosis. Cells were plated onto 12-well plates (Falcon) and after 12 hours were subjected to different concentrations of recombinant human TGF-β cytokine (PeproTech) which was replaced every 3 days. After approximately 10 days, the cells were stained with crystal violet dye. The statistical quantification was analyzed by gray density values using Image J software.

GST pull-down assay

The coding sequence of different Smads were cloned into a pEGX-4T-2 vector to form GST fusion proteins. GST fusion proteins were immobilized on glutathione-S-Sepharose beads (Amersham Biosciecces). After washing with a pull-down buffer (20 mm Tris-HCl, pH 7.5, 150 mm NaCl, 0.1% Nonidet P-40, 1 mm dithiothreitol, 10% glycerol, 1 mm EDTA, 2.5 mm $MgCl_2$, and 1 μg/ml leupeptin), the beads were incubated with cell lysates from 293T cells express-

ing Myc-tagged HEY2 for 4 hours at 4°C. The sepharose beads were then washed 5 times with binding buffer and resuspended in sample buffer. The bound proteins were analyzed by western blot.

Immunoprecipitation

293T cells were transfected with the indicated plasmids and lysed at 24 hours post-transfection with cold lysis buffer [5 mM EDTA, 0.5% NP-40, 0.1 mM phenylmethane sulphonylflouride (PMSF), 10 μM pepstatin A, 10 μM leupeptin and 25 μg/ml aprotinin]. The lysate was centrifuged and the suspenatant was precleared by protein G Plus/protein A agarose beads (Amersham Biosciecces) for 1 hour. Then, pre-cleared cell lysates were incubated with 1 μg anti-myc mono-clonal antibody (mAb) and G Plus/protein A agarose beads for 6 hours. All the processes were performed at 4°C with rotation. The final agarose beads were washed 5 times with lysis buffer and resuspended in sample buffer and analyzed by western blotting.

Luciferase reporter assay

The luciferase reporters, including of DR5-Luc, NFAT-Luc, E2F-Luc, Rb-Luc, p53-Luc, AP1-Luc, CRE-Luc, SRE-Luc, GRE-Luc and HSE-Luc, were purchased from Clontech Inc. The luciferase reporter of SBE-Luc was kindly provided by Dr. Robert P. Coppes (University of Groningen). c-Myc promoter luciferase reporter (c-Myc promoter-Luc) was constructed by our lab. A region of the c-Myc promoter (nucleotides -2206 to +196) harboring the TGF-β inhibitory element (TIE) was generated by PCR and subcloned into the pGL3-Basic vector (Promega) to form c-Myc promoter-Luc.

Hep3B cells were co-transfected with the indicated firefly luciferase reporter construct, pRL-SV40 (internal control reporter vector) and observed gene expression constructs (Smad3, Smad4 and HEY2) and/or with an empty vector. Luciferase activities were determined using the Dual Luciferase reporter system (Promega) on a Lumat LB 9507 luminometer (Berthold). Values were normalized with the renilla luciferase activity of pRL-SV40. Each assay was performed in triplicate.

Immunofluorescence microscopy

Cells cultured and transiently transfected on coverslips were fixed with 4% paraformaldehyde for 10 minutes and permeabilized with 0.2% Triton X-100 for 5 minutes at room temperature. Cells were washed 3 times with TBS (50 mM Tris-HCl pH 7.4, 150 mM NaCl) and blocked with 10% normal horse serum plus 1% BSA (Amersham Biosciences, USA) for 1 hour. Cells then were incubated with a combination of mouse anti-Myc antibody (1:200 dilution) and rabbit anti-HA antibody (1:200 dilution) at 4°C overnight. After being washed 3 times in TBS containing 0.1% Tween-20, the cells were incubated with Alexa Fluor 555 goat anti-mouse IgG antibody (1:500 dilution) and Alexa Fluor 488 goat anti-rabbit IgG antibody (1:500 dilution) for 1 hour and stained with DAPI for 15 minutes. Confocal microscopy analysis was performed using a LSM700 laser scanning microscope (Carl Zeiss).

Results

HEY2 in neoplastic cytoplasm was up-regulated in HCC

HEY2 protein expression in HCCs was analyzed by western blot and immunohistochemistry (IHC) assays. Western blot analysis revealed that HEY2 protein was detected readily in the majority of HCC cell lines examined (Hep3B, HepG2, Huh7, SMMC-7721 and SK-Hep1) (**Figure 1A**). Next, proteins extracted from 11 paired HCC tissues were subjected to western blot. HEY2 protein was up-regulated in 9 out of 11 HCC tissues compared to the adjacent noncancerous tissues (**Figure 1B**). To further determine the expression pattern of HEY2 in HCC tissues, immunohistochemical analyses of tissue microarray with 90 paired HCCs (180 samples) were performed (Figure S1). The antibody used in this IHC assay was human HEY2 antibody (NBP1-88629, Novus, 1:300), which can recognize endogenous and overexpressed HEY2 in a single band as demonstrated by western blot analysis in many types of cancer cell (293T, Hela, U87, A549 and 7860) (Figure S2). The staining pattern showed that HEY2 was expressed both in the cytoplasm and nucleus (mainly in nucleus), and HEY2 was expressed mainly in neoplastic cells, and it also was expressed in stromal cells and inflammatory cells of tumor and surrounding non-cancer-

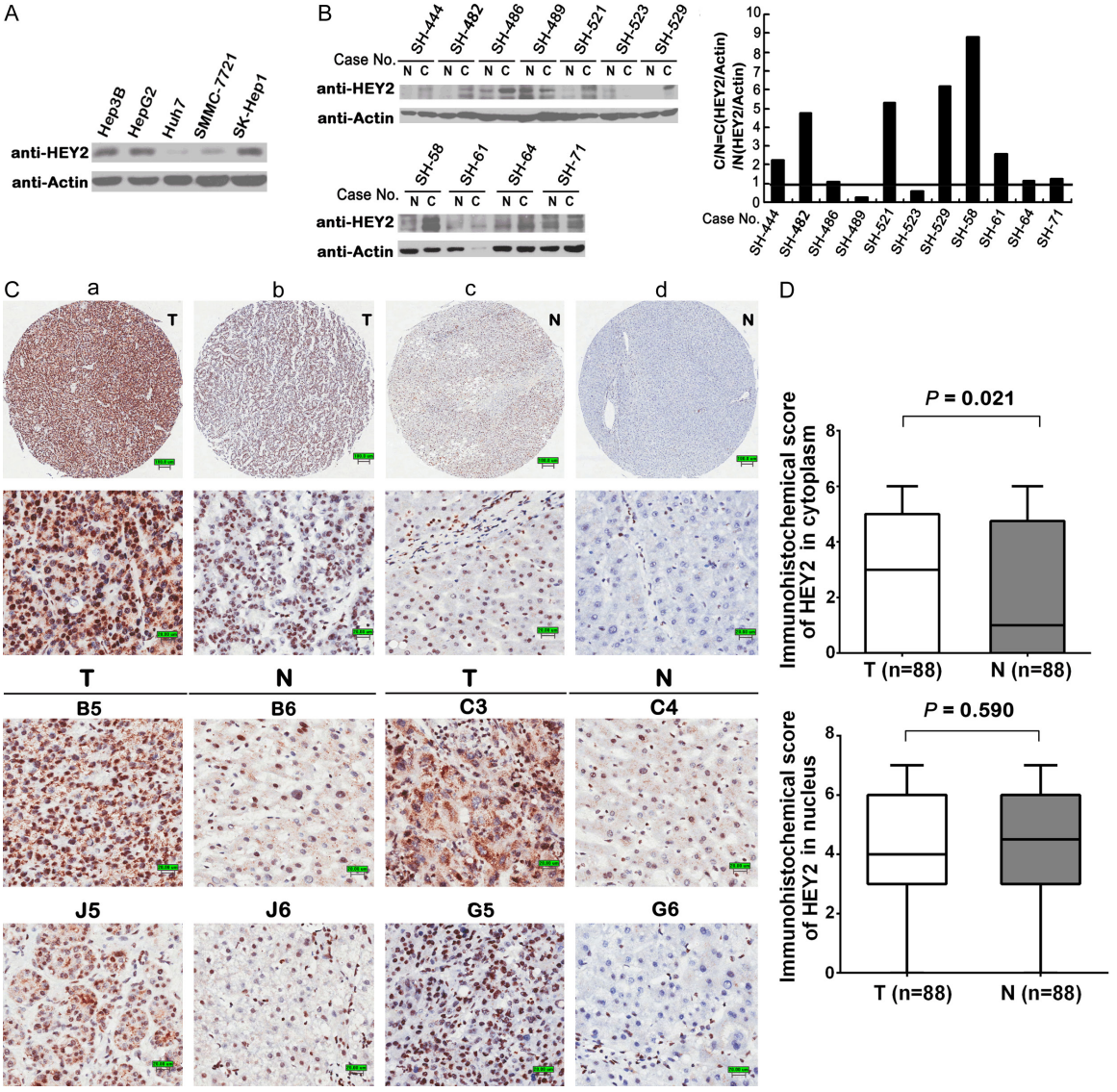

Figure 1. Cytoplasmic HEY2 protein is up-regulated in HCC. A. Expression of HEY2 protein in five HCC cell lines was examined by western blot. B. HEY2 protein expression levels were analyzed in 11 paired HCCs and their corresponding non-cancerous tissues by western blot. Fold change of HEY2 protein with respect to non-cancerous specimens were normalized to β-actin. The quantification of immunoblots was shown in the right panel. N, non-cancerous tissue; C, primary HCC tissue. C. Representative HEY2 staining in HCC tissue (C) and adjacent non-cancerous tissue (N). a. Tumor tissue showing strong positive staining (plasma Q-score = 6, nucleus Q-score = 7); b. Tumor tissue showing moderate staining (plasma Q-score = 0, nucleus Q-score = 5); c. Non-cancerous tissue showing moderate staining (plasma Q-score = 0, nucleus Q-score = 4); d. Non-cancerous tissue showing negative staining (Plasma Q-score = 0, Nucleus Q-score = 0). The representative HEY2 staining in 4 paired HCC tissues (C) and adjacent non-cancerous tissues (N) as shown in lower panel. Scale bar = 20 μm. D. The IHC score (Q-score) of HEY2 in cytoplasm (up panel) or in nucleus (lower panel) of 88 HCC patients was indicated by the box plot (Whiskers, 25-75 percentiles) and the wilcoxon matched paired test was used to calculate the *P* value.

ous tissues (**Figure 1C**). Particularly, HEY2 was detected more in the neoplastic cytoplasm than in non-cancerous cytoplasm (**Figure 1C** lower panel). To determine the significance of HEY2 expression in HCC and adjacent non-cancerous tissues. HEY2 expression status of each sample was quantified in the cytoplasm and nucleus by the Quick score (Q-score) method. The numbers of patients with respect to the intensity and distribution of HEY2 staining were shown in Table S2. When comparing the IHC score of HEY2 expression between HCC and

Table 1. Correlation of the clinicopathological characteristics with tumor HEY2 expression in cytoplasm

Variable	HEY2 Expression in cytoplasm			
	Total, n (%)	Q-score ≤4, n (%)	Q-score >4, n (%)	*P* value
Q-score	90 (100)	56 (62)	34 (38)	
Sex†				
Female	81 (90)	51 (63)	30 (37)	0.725
Male	9 (10)	5 (56)	4 (44)	
Age-yr				
<55	47 (31)	29 (62)	18 (38)	0.984
≥55	42 (69)	26 (62)	16 (38)	
Missing	1			
Tumor size				
<5 cm	35 (39)	21 (60)	14 (40)	0.646
≥5 cm	54 (61)	35 (65)	19 (35)	
Missing	1			
Pathological differentiation				0.044*
I-II	57 (63)	31 (54)	26 (46)	
III-IV	33 (37)	25 (76)	8 (24)	
TNM clinical stage				
I-II	40 (49)	22 (55)	18 (45)	0.526
III-IV	42 (51)	26 (62)	16 (38)	
Missing	8			

*$P<0.05$, †Fisher's exact test was used.

adjacent non-cancerous tissues, 2 patients were excluded since the non-cancerous tissues were missing. Result of immunohistochemistry staining in 88 patients with HCC showed a significant increase of cytoplasmic HEY2 expression in tumor tissues ($P = 0.021$) (**Figure 1D** up panel), but no difference of nuclear HEY2 expression was found between tumor tissues and adjacent non-cancerous tissues ($P = 0.590$) (**Figure 1D** lower panel). Data taken from western blot and immunohistochemical analyses indicate that increased HEY2 expression in neoplastic cytoplasm, is prevalent in patients with HCC.

To evaluated the relevance of HEY2 expression with clinicopathological characteristics of the HCC patients, a score of 4 was used as the cut-off value to define the expressional abundance of HEY2 (high level with a Q-score >4 and low level with a Q-score ≤4). As shown in **Table 1**, the expression status of HEY2 in neoplastic cytoplasm was significantly associated with pathological differentiation ($P = 0.044$), but not in the neoplastic nucleus ($P = 0.769$) (Table S3). No correlation was observed between HEY2 expression and tumor size, clinical stages, gender and age of patients, both in the neoplastic cytoplasm and the neoplastic nucleus.

HEY2 inhibits TGF-β-induced HCC growth inhibition

To determine the biological significance of HEY2, we established HEY2-overexpressing stable clones (E5 and E9) and control clones (P1 and P2) of Hep3B cells, confirmed by western blot analysis (**Figure 2A**). MTS assay showed that overexpression of HEY2 had negligible effects on growth of Hep3B cells and only a significant difference of growth rate between HEY2-overexpressing and control cells was observed at day 7 (**Figure 2B**). Loss-of-function approach was also used to assess the role of HEY2 in HCC cell growth. The HEY2-targeting siRNAs were designed and confirmed with western blot (**Figure 2C**). In agreement with the data shown in **Figure 2B**, knockdown of HEY2 had a slight inhibitory effect on cell growth (**Figure 2D**).

Cytokines in the tumor microenvironment play an important role in tumor occurrence and progress. We hypothesize that HEY2 may exert function in certain conditions. The dual-luciferase reporter assay was used to investigate the potential signaling pathways in which HEY2 involved. As shown in **Figure 3A**, ectopic expression of HEY2 significantly decreased SBE-luc luciferase activity, with an inhibitory rate of 53% ($P = 0.021$). HEY2 also had significantly, but minimal effect on GRE-luc luciferase activity with an inhibitory rate of 24% ($P = 0.024$). HEY2 expression had no effect on other Luc-reporters (DR5-luc, NFAT-luc, E2F-luc, Rb-luc, P53-luc, AP1-luc, CRE-luc, SRE-luc and HSE-luc). SBE (Smad binding element) was a specific downstream responsive element for the TGF-β/Smads signaling pathway and TGF-β is a critical pleiotrophin in the tumor microenvironment. Therefore, we next investigated the biological significance of HEY2 in TGF-β-induced cell-growth arrest by using MTS and colony formation assays. Compared with cell growth in nor-

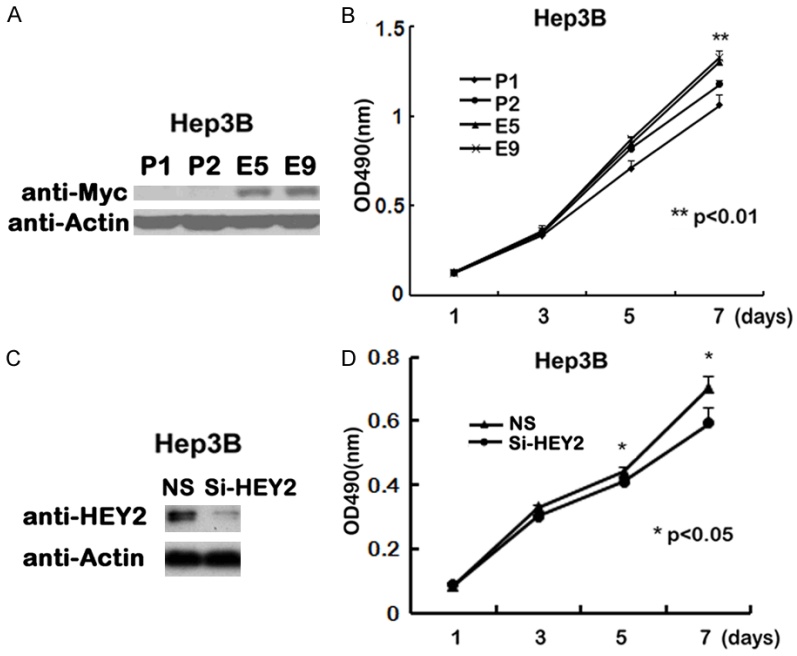

Figure 2. HEY2 inhibited HCC growth as a weak effect. A. Two HEY2-overexpressing stable clones (E5, E9) of Hep3B cells and two control clones (P1 and P2) were identified by western blot. B. Effect of HEY2 overexpression on the proliferation of Hep3B cells, as measured every 2 days by MTS assay. Data are presented with the means ± standard deviation (n = 5); $^{**}P<0.01$. C. Hep3B cells were transfected with HEY2 specific siRNA (Si-HEY2) or non-specific siRNA (NS) and analyzed by western blot. D. Effect of HEY2 knockdown on proliferation of Hep3B cells, as measured every 2 days by MTS assay. Data are presented with the means ± standard deviation (n = 5); $^{*}P<0.05$.

mal conditions, treatment with TGF-β extremely decreased Hep3B cell growth, as detected by MTS assay. In agreement with the data shown in **Figure 2B**, the effect of HEY2 on Hep3B cell growth was negligible, with a significant difference only seen at day 7 under normal growth conditions (**Figure 3B**, left, P1 and P2 vs. E5 and E9). However, when treated with TGF-β, HEY2-overexpressing stable clones (E5 and E9) obviously and significantly blocked TGF-β-induced cell growth arrest and growth faster than control clones (P1 and P2) (**Figure 3B**, right). In colony formation assay, considering that long-term stimulation of TGF-β would cause cell cycle arrest and apoptosis, high cell density was used in colony formation assays and overall colony gray density value was employed to reflect cell growth capability. As shown in **Figure 3C**, HEY2 overexpression had negligible effect on cell colony formation without TGF-β treatment, whereas resulted in the formation of significantly more and larger colonies compared to control clones when treated with 2 ng/ml of TGF-β (**Figure 3C**, E5 and E9 vs. P1 and P2).

In agreement with the data shown in **Figure 2D**, knockdown of HEY2 had a slight inhibitory effect on cell growth without TGF-β treatment (**Figure 3D**, left). When treated with TGF-β (2 ng/ml), knockdown of HEY2 apparently and significantly promoted the suppressive effect of TGF-β on cells growth (**Figure 3D**, right) and this effect was in a time-dependent manner. HEY2-induced suppression was 0.279 at day 5 and 0.313 at day 7, compared to 0.357 at day 5 and 0.583 at day 7 in the control cells. The cell colony formation assay further showed that knockdown of HEY2 in Hep3B cells resulted in fewer and smaller colonies compared with the control cells both in normal condition and in condition of treatment with TGF-β (**Figure 3E**). Taken together, these results indicate the potential role of HEY2 in TGF-β-induced growth arrest of HCC cells.

HEY2 inhibits the TGF-β-induced downregulation of c-Myc

Downregulation of c-Myc is a critical event in TGF-β-induced growth arrest. TGF-β reduces c-Myc transcription, resulting in the stimulation of the expression of p21 and p15 and then cell cycle arrest [40, 41]. Therefore, we next investigated the role of HEY2 in regulating the transcription of TGF-β/Smad downstream target genes. As shown in **Figure 4A** and **4B**, TGF-β-induced decrease of c-Myc mRNA in Hep3B cells (A) or HepG2 cells (B) was slower in HEY2 transient over-expressed cells compared with control cells. Consistently, TGF-β-induced increase of p21 and p15 mRNA was also attenuated by HEY2 expression in Hep3B cells (**Figure 4C** and **4D**), which confirmed the HEY2 effect on c-Myc transcription. Further, we examined

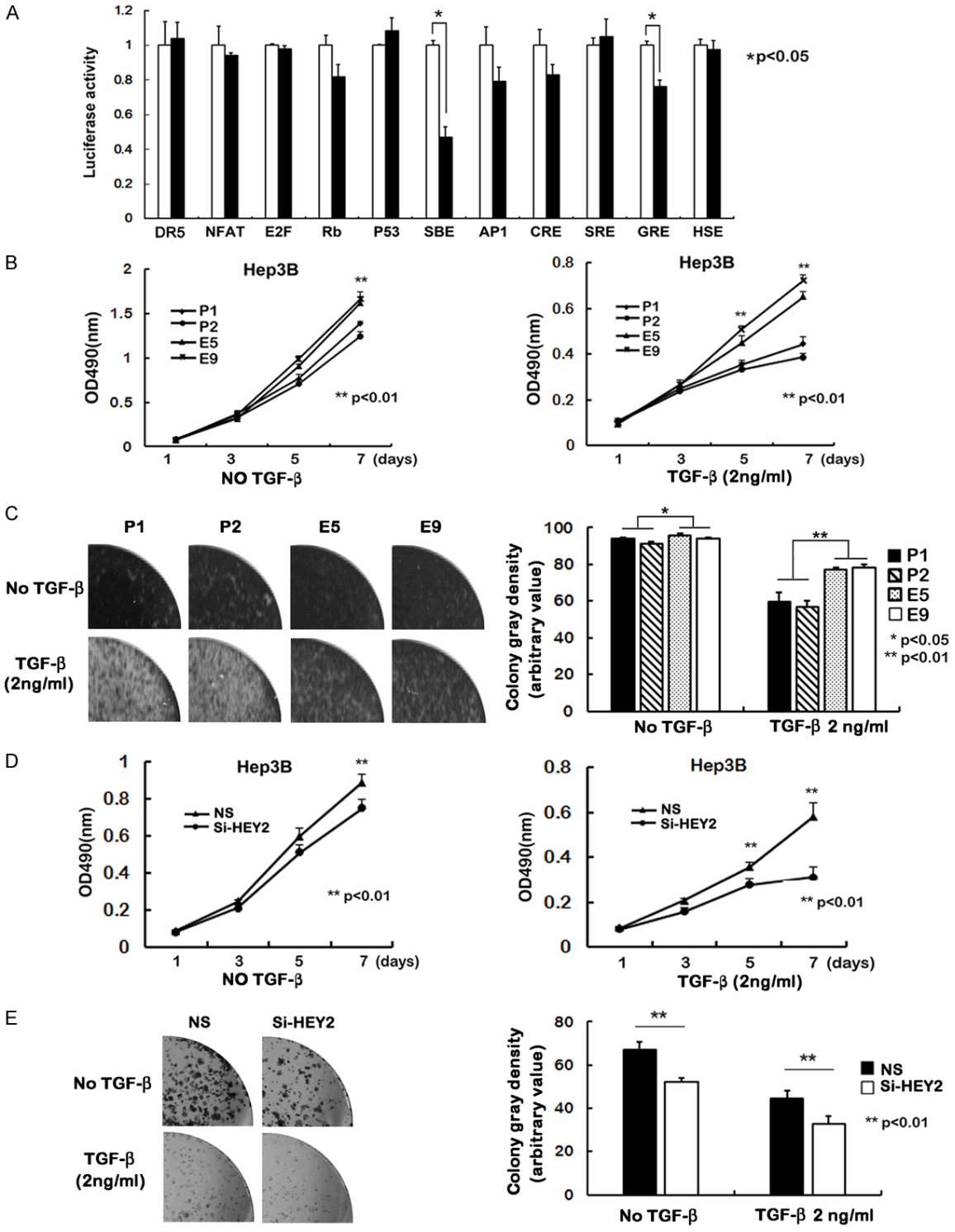

Figure 3. HEY2 blocked TGF-β-induced HCC growth inhibition. A. Hep3B cells were transfected with the indicated luciferase pathway reporter, pRL-SV40 (internal control), and Myc-HEY2 or with the empty vector. After 24 hours, the luciferase activities were measured by a luminometer. Error bars, ± standard deviation from triplicates. *P<0.05. B. Effect of stable overexpression of HEY2 on the proliferation of Hep3B cells without TGF-β (left panel) or with 2 ng/ml TGF-β (right panel) incubation for 7 days, as measured every 2 days by MTS assay. Data are presented with the means ± standard deviation (n = 5); **P<0.01. C. Stable cell lines were plated into 12-well plates at a density of 4K cells/well and incubated with or without 2 ng/ml TGF-β for 10 days. Representative photographs of cell colonies were shown. The statistical quantification was analyzed by gray density values using Image J software (right panel).

Error bars, ± standard deviation from three random areas; *P<0.05, **P<0.01. D. Effect of HEY2 knockdown on proliferation of Hep3B cells incubated with or without 2 ng/ml TGF-β for 7 days, as measured every 2 days by MTS assays. Data are presented with the means ± standard deviation (n = 5); **P<0.01. E. Hep3B cells were transfected with siRNA against HEY2 or control. After 24 hours, siRNA transfected cells were plated into 12-well plates at a density of 2K cells/well and incubated with or without 2 ng/ml TGF-β for 10 days. Representative photographs of cell colonies were shown. The statistical quantification was analyzed by gray density values using Image J software (right panel). Error bars, ± standard deviation from three random areas; **P<0.01.

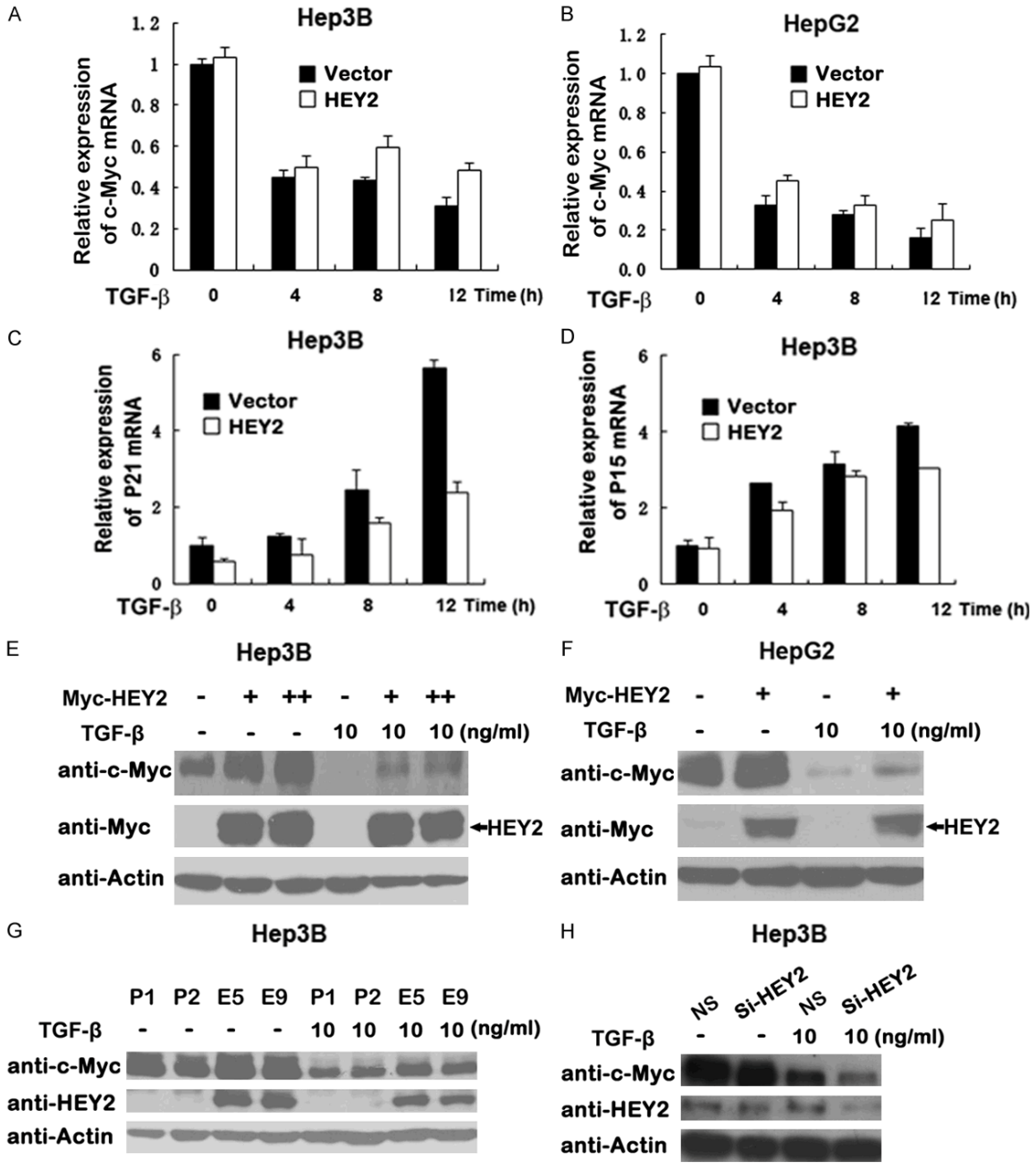

Figure 4. HEY2 inhibited the TGF-β-induced downregulation of c-Myc. (A, B) Effect of HEY2 overexpression on TGF-β-induced downregulation of c-Myc mRNA level in Hep3B cells (A) and HepG2 cells (B). Cells transfected with HEY2 or control plasmids were starved in 1% serum for 6 hours and then treated with TGF-β (10 ng/ml) for the indicated length of time. Equal amounts of cell lysates at each time point were subjected to real-time PCR. Error bars, ± standard deviation from triplicates. (C, D) Effect of HEY2 overexpression on TGF-β-induced upregulation of p21 mRNA expression (C) and p15 mRNA expression (D) in Hep3B cells, analyzed by the same method mentioned above. (E, F)

Effect of HEY2 overexpression on c-Myc protein expression in Hep3B cells (E) and HepG2 cells (F). Cells transfected with HEY2 or control plasmids were treated with or without 10 ng/ml TGF-β for 24 hours. The endogenous c-Myc protein levels were detected by western blot. (G) HEY2-overexpressing stable clones (E5, E9) and control clones (P1 and P2) of Hep3B cells were incubated with or without 10 ng/ml TGF-β for 24 hours and cell lysates was analyzed by western blot with indicated antibodies. (H) Effect of HEY2 knockdown on c-Myc protein expression in Hep3B cells. Cells were transfected with HEY2 specific siRNA (Si-HEY2) or non-specific siRNA (NS). At 24 hours post-transfection, cells were incubated with or without 10 ng/ml TGF-β for 24 hours and cell lysates was subjected to western blot with indicated antibodies.

the effect of HEY2 on c-Myc protein expression. As shown in **Figure 4E** and **4F**, transient transfection of HEY2 could promote the c-Myc protein expression in Hep3B cells (E) and HepG2 cells (F). Treatment with TGF-β extremely reduced c-Myc protein level, whereas ectopic expression of HEY2 obviously inhibited TGF-β-induced downregulation of c-Myc. This effect was also confirmed in HEY2-overexpressing stable clones of Hep3B cells (**Figure 4G**). Moreover, knockdown of endogenous HEY2 via HEY2-specific siRNA decreased the expression of c-Myc and promoted TGF-β-induced downregulation of c-Myc compared with that in the control cells (**Figure 4H**).

HEY2 represses Smad3 and Smad4 transcriptional activity through association with Smad3 and Smad4

As discussed above, HEY2 significantly decreased activity of SBE (Smad binding element) luciferase reporter. One of the possibilities is that HEY2 may interact with Smads and interfere with their transcriptional activity. Therefore, we sought to identify whether HEY2 could interact with different Smads using the Pull-down assay. Recombinant GST-Smad1, GST-Smad2, GST-Smad3, GST-Smad4 and GST-Smad5 proteins were expressed and purified from bacteria. Myc-HEY2 was transfected in 293T cells and a protein sample was harvested. As shown in **Figure 5A**, GST-Smad3 and GST-Smad4 strongly bound to Myc-HEY2 in a Pull-down assay. GST-Smad5 combined weakly with HEY2 while other GST-Smads examined did not combine with HEY2. To determine whether HEY2 interacts with Smad3 and Smad4 in human cells, we co-expressed Myc-HEY2 and HA-Smad3, or Myc-HEY2 and HA-Smad4 in 293T cells and immuno-precipitated HEY2 using anti-Myc antibodies. Results showed that both HA-Smad3 and HA-Smad4 co-immunoprecipitated with HEY2 (**Figure 5B**). To further confirm the interaction between Smad3 and HEY2, or Smad4 and HEY2 in vivo, we determined whether these two proteins are co-localized to the same subcellular compartments. As shown in **Figure 5C**, when HA-Smad3 and Myc-HEY2 were co-expressed in Hela cells, two proteins were co-localized in the nucleus. Smad4 and HEY2 were also shown to co-localized in the nucleus using the same assay.

Based on the findings above, we next examined the effects of HEY2 on Smad3 and Smad4 (Smad3/4) transcriptional activity. We employed the SBE-Luc as Smad3/4-activating luciferase reporter and c-Myc promoter-Luc harboring the TGF-β inhibitory element (TIE) as Smad3/4-repressing luciferase reporter, to investigate the effects of HEY2 on Smad3/4 transcriptional activity. As shown in **Figure 5D** and **5E**, the increase of SBE-luc reporter activity induced by Smad3/4 and the decrease of c-Myc promoter-Luc reporter activity induced by Smad3/4 were both repressed by the HEY2 expression in a dose-dependent manner.

Taken together, these results suggest that HEY2 may play a crucial role in mediating TGF-β/Smad pathway in HCC tumorigenesis.

Discussion

Findings from our present study unravel a novel function of HEY2 in the TGF-β/Smad pathway (**Figure 5F**). The model suggests the potential molecular mechanism underling the oncogenic role of HEY2 in HCC tumorigenesis. Our results demonstrated that HEY2, a bHLH dmain-containing transcription factor, acted as a co-repressor with Smad3/4 to inhibit TGF-β-induced downregulation of c-Myc and then inhibit TGF-β-induced growth arrest of HCC cell. Loss of TGF-β growth inhibitory effect is one of the key issues in tumorigenesis [4]. Smads are central mediators of signals from the receptors for TGF-β superfamily members to the nucleus [15, 42]. Several transcriptional co-repressors have been shown to shift Smads-mediated signaling from tumor suppression to oncogenesis. Ski

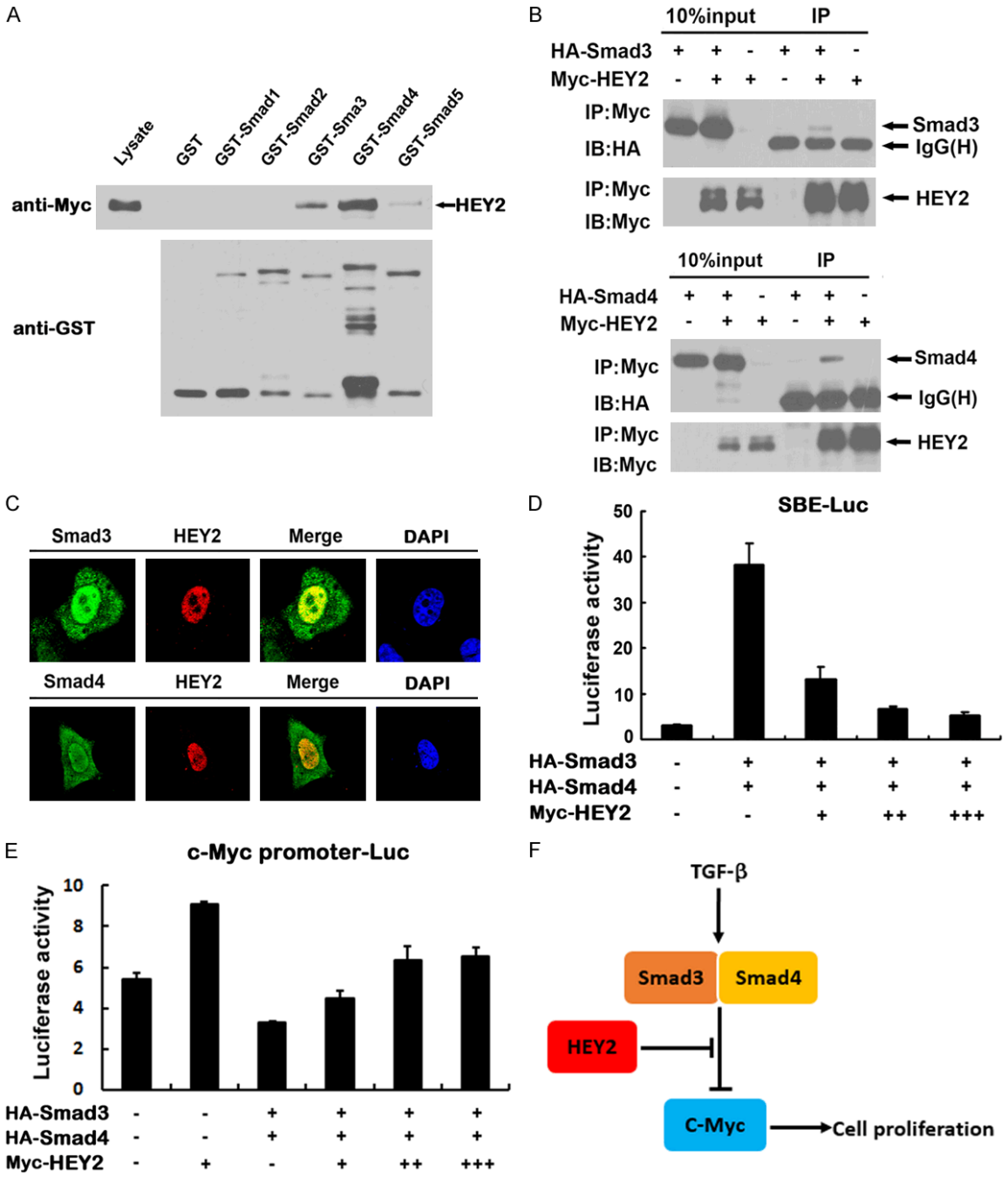

Figure 5. HEY2 repressed Smad3/4 transcriptional activity through its association with Smad3/4. A. Bacterially expressed GST and various GST-Smad fusion proteins were bound to glutathione-Sepharose beads, and then were incubated to Myc-HEY2 protein. Bound Myc-HEY2 proteins were detected by western blot using anti-Myc antibody. B. Myc-HEY2 was co-transfected with the same amount of Smad3 (left panel) or Smad4 (right panel) into 293T cells. After 24 hours, cell lysates were prepared and subjected to immunoprecipitation with anti-Myc antibodies. The immunoprecipitates (IP) were analyzed by western blot with either anti-HA or anti-Myc antibodies. C. Myc-HEY2 was co-transfected with HA-Smad3 or Smad4 into Hela cells. Fluorescent micrographs showed the localization of Smad3 (green) and HYE2 (red) (up panel), and also Smad4 (green) and HYE2 (red) (lower panel). D. Effect of HEY2 on Smad3/4-activating luciferase reporter (SBE-Luc). Hep3B cells were transfected with the SBE-luc, pRL-SV40, Smad3 and Smad4 vectors, and increasing amount Myc-HEY2 (0, 10, 20 or 50 ng) or with the empty vector. After 24 hours, the luciferase activities were measured by a luminometer. Error bars, ± standard deviation from triplicates. E. Effect of HEY2 on Smad3/4-repressing luciferase reporter (c-Myc promoter-Luc). Hep3B cells were transfected with the c-Myc promoter-Luc, pRL-SV40, Smad3 and Smad4 vectors, and increasing amount Myc-HEY2 (0, 10, 20 or 50 ng) or with the empty vector as indicated. After 24 hours, the luciferase activities were measured by a luminometer. Error bars, ± standard deviation from triplicates. F. A model depicting the HEY2-mediated TGF-β response by interfering with Smad3/4 transcriptional activity.

and SnoN are Smad-interacting proteins that negatively regulate the TGF-β signaling pathway by disrupting the formation of R-Smad/Smad4 complexes, as well as by inhibiting Smad association with the p300/CBP coactivators [43-45]. Besides, Battaglia et al. [46] indicate that the HCV core protein may switch TGF-β growth inhibitory effects to tumor promoting responses by decreasing Smad3 activation. In this study, we showed that HEY2 blocked TGF-β growth inhibitory activity by associating with Smad3 and Smad4 and repressing their transcriptional activity. HEY2 may act as another possible transcriptional repressor to make HCC cell unresponsive to TGF-β growth inhibitory effect.

HEY2 gene are previously found to be target of Notch signaling [21, 25], and have pro-oncogenic role in human cancers. Downregulation of HEY2 mediated by knockdown of Notch2 inhibits cell proliferation, invasion, and migration in salivary adenoid cystic carcinoma [47]; Upregulation of HEY2 induced by Notch activation is associated with chemoresistance to trastuzumab in gastric cancer cells [48]. HEY2 is also found to promote cell proliferation and migration in hepatocellular carcinoma [35]. In agreement with these findings, we showed that cytoplasmic HEY2 protein was up-regulated in HCC, and HEY2 could block TGF-β-induced growth inhibitory effect on HCC cells. TGF-β is a critical pleiotrophin in the tumor microenvironment. Therefore, our results confirm the oncogenic role of HEY2 in HCC and furtherly reveal the significance of HEY2 in regulating tumor cells to cope with microenvironmental stress during HCC tumorigenesis.

One interesting phenomenon is that HEY2 protein in tumor cytoplasm was up-regulated in HCC (**Figure 1D**). One possible explanation is that increased cytoplasmic HEY2 might competitively disrupt the association of Smad3/4 with other co-transcriptional factors in cytoplasm, resulting in dysfunction of TGFβ signaling pathway and HCC cell growth. Previously study indicates that HEY2 was up-regulated in HCC [35]. However, our result from tissue microarray with 90 paired HCCs showed that HEY2 in neoplastic cytoplasm was up-regulated in HCC while not the nuclear HEY2 expression. Different sample sizes and different histochemical scoring methods might contribute to these different findings. Although cytoplasmic expression status of HEY2 shows significant association with pathological differentiation, it is regretful that we failed to collect adequate information for clinical and pathologic characteristics. Future studies are necessary to investigate the relevance of HEY2 with more complete and comprehensive clinicopathological characteristics.

The HEY family consists of three members including HEY1, HEY2, and HEY-Like (HEYL). HEY proteins share homology in their bHLH regions, which mediate DNA binding and dimerization, as well as in an Orange domain and a conserved but different C-terminal YXXW-TE(I/V)GAF domain, in which the KPYRPWG motif in HEY1 is modified to KPYQPWG in HEY2 and is absent in HEYL [23, 49]. We also examined the interaction between all three HEY family members (HEY1, HEY2, HEYL) and Smad3, and found that HEY2 and HEYL associated with Smad3 while HEY1 did not (Figure S3). This result suggests that each member of the HEY family might exert its function by distinct mechanisms.

In conclusion, our findings suggest a novel role of HEY2 in resisting TGF-β growth inhibitory effects in HCC. Shift of TGF-β/Smad signaling from tumor suppression to oncogenesis is one of the key issues in tumorigenesis. Our results provide a possible reference for the mechanism of this shift process, which may contribute to the improvement of diagnosis and molecular targeted therapy for HCC.

Acknowledgements

This work was supported by the National Natural Science Foundation (Grant # 81402297 to QYX) and partially funded by the Key Project of the Fourth-Round Three-Year Plan of Action on Public Health in Shanghai (grant no. 15GWZK1001). We thank all participants who agreed to participate in this study.

Disclosure of conflict of interest

None.

Abbreviations

TGF-β, transforming growth factor-beta; HCC, hepatocellular carcinoma; HEY2, The Hairy and

Enhancer of Split-related with YRPW motif 2; siRNA, small interfering RNA; IHC, immunohistochemistry; TMA, tissue microarray.

Address correspondence to: Dr. Qianyi Xiao, Department of Preventive Medicine, Key Laboratory of Public Health Safety of The Ministry of Education, School of Public Health, Fudan University, 138 Yixueyuan Rd, Shanghai 200032, China. Tel: +86-21-54237448; Fax: +86-21-54237448; E-mail: xiaoqianyi@fudan.edu.cn

References

[1] Torre LA, Bray F, Siegel RL, Ferlay J, Lortet-Tieulent J and Jemal A. Global cancer statistics, 2012. CA Cancer J Clin 2015; 65: 87-108.

[2] Massague J, Blain SW and Lo RS. TGFbeta signaling in growth control, cancer, and heritable disorders. Cell 2000; 103: 295-309.

[3] Roberts AB and Wakefield LM. The two faces of transforming growth factor beta in carcinogenesis. Proc Natl Acad Sci U S A 2003; 100: 8621-8623.

[4] Meulmeester E and Ten DP. The dynamic roles of TGF-beta in cancer. J Pathol 2011; 223: 205-218.

[5] Drabsch Y and Ten DP. TGF-beta signalling and its role in cancer progression and metastasis. Cancer Metastasis Rev 2012; 31: 553-568.

[6] Senturk S, Mumcuoglu M, Gursoy-Yuzugullu O, Cingoz B, Akcali KC and Ozturk M. Transforming growth factor-beta induces senescence in hepatocellular carcinoma cells and inhibits tumor growth. Hepatology 2010; 52: 966-974.

[7] Damdinsuren B, Nagano H, Kondo M, Natsag J, Hanada H, Nakamura M, Wada H, Kato H, Marubashi S, Miyamoto A, Takeda Y, Umeshita K, Dono K and Monden M. TGF-beta1-induced cell growth arrest and partial differentiation is related to the suppression of Id1 in human hepatoma cells. Oncol Rep 2006; 15: 401-408.

[8] Carmona-Cuenca I, Roncero C, Sancho P, Caja L, Fausto N, Fernandez M and Fabregat I. Upregulation of the NADPH oxidase NOX4 by TGF-beta in hepatocytes is required for its pro-apoptotic activity. J Hepatol 2008; 49: 965-976.

[9] Bissell DM. Chronic liver injury, TGF-beta, and cancer. Exp Mol Med 2001; 33: 179-190.

[10] Yang ZX, Wang H, Gao CF, Xu LL and Zhao WJ. Effect of polymorphism of transforming growth factor beta1 gene on HBV-induced liver cirrhosis. Zhonghua Yi Xue Za Zhi 2005; 85: 1021-1026.

[11] Thiery JP and Sleeman JP. Complex networks orchestrate epithelial-mesenchymal transitions. Nat Rev Mol Cell Biol 2006; 7: 131-142.

[12] Yang YA, Zhang GM, Feigenbaum L and Zhang YE. Smad3 reduces susceptibility to hepatocarcinoma by sensitizing hepatocytes to apoptosis through downregulation of Bcl-2. Cancer Cell 2006; 9: 445-457.

[13] Heldin CH and Moustakas A. Role of Smads in TGFbeta signaling. Cell Tissue Res 2012; 347: 21-36.

[14] Massague J and Wotton D. Transcriptional control by the TGF-beta/Smad signaling system. EMBO J 2000; 19: 1745-1754.

[15] Zimmerman CM and Padgett RW. Transforming growth factor beta signaling mediators and modulators. Gene 2000; 249: 17-30.

[16] Chen CR, Kang Y and Massague J. Defective repression of c-myc in breast cancer cells: a loss at the core of the transforming growth factor beta growth arrest program. Proc Natl Acad Sci U S A 2001; 98: 992-999.

[17] Yagi K, Furuhashi M, Aoki H, Goto D, Kuwano H, Sugamura K, Miyazono K and Kato M. c-myc is a downstream target of the Smad pathway. J Biol Chem 2002; 277: 854-861.

[18] Henriksson M and Luscher B. Proteins of the Myc network: essential regulators of cell growth and differentiation. Adv Cancer Res 1996; 68: 109-182.

[19] Usa T, Tsukazaki T, Namba H, Ohtsuru A, Kimura H, Villadolid MC, Nagataki S and Yamashita S. Correlation between suppression of c-myc and antiproliferative effect of transforming growth factor-beta 1 in thyroid carcinoma cell growth. Endocrinology 1994; 135: 1378-1384.

[20] Baldwin RL, Tran H and Karlan BY. Loss of c-myc repression coincides with ovarian cancer resistance to transforming growth factor beta growth arrest independent of transforming growth factor beta/Smad signaling. Cancer Res 2003; 63: 1413-1419.

[21] Iso T, Kedes L and Hamamori Y. HES and HERP families: multiple effectors of the Notch signaling pathway. J Cell Physiol 2003; 194: 237-255.

[22] Fischer A and Gessler M. Delta-Notch--and then? Protein interactions and proposed modes of repression by Hes and Hey bHLH factors. Nucleic Acids Res 2007; 35: 4583-4596.

[23] Nakagawa O, Nakagawa M, Richardson JA, Olson EN and Srivastava D. HRT1, HRT2, and HRT3: a new subclass of bHLH transcription factors marking specific cardiac, somitic, and pharyngeal arch segments. Dev Biol 1999; 216: 72-84.

[24] Leimeister C, Externbrink A, Klamt B and Gessler M. Hey genes: a novel subfamily of hairy- and Enhancer of split related genes specifically expressed during mouse embryogenesis. Mech Dev 1999; 85: 173-177.

[25] Nakagawa O, McFadden DG, Nakagawa M, Yanagisawa H, Hu T, Srivastava D and Olson EN. Members of the HRT family of basic helix-loop-helix proteins act as transcriptional repressors downstream of Notch signaling. Proc Natl Acad Sci U S A 2000; 97: 13655-13660.
[26] Xin M, Small EM, van Rooij E, Qi X, Richardson JA, Srivastava D, Nakagawa O and Olson EN. Essential roles of the bHLH transcription factor Hrt2 in repression of atrial gene expression and maintenance of postnatal cardiac function. Proc Natl Acad Sci U S A 2007; 104: 7975-7980.
[27] Kathiriya IS, King IN, Murakami M, Nakagawa M, Astle JM, Gardner KA, Gerard RD, Olson EN, Srivastava D and Nakagawa O. Hairy-related transcription factors inhibit GATA-dependent cardiac gene expression through a signal-responsive mechanism. J Biol Chem 2004; 279: 54937-54943.
[28] Iso T, Sartorelli V, Poizat C, Iezzi S, Wu HY, Chung G, Kedes L and Hamamori Y. HERP, a novel heterodimer partner of HES/E(spl) in Notch signaling. Mol Cell Biol 2001; 21: 6080-6089.
[29] Fischer A, Schumacher N, Maier M, Sendtner M and Gessler M. The Notch target genes Hey1 and Hey2 are required for embryonic vascular development. Genes Dev 2004; 18: 901-911.
[30] Kokubo H, Miyagawa-Tomita S, Nakazawa M, Saga Y and Johnson RL. Mouse hesr1 and hesr2 genes are redundantly required to mediate Notch signaling in the developing cardiovascular system. Dev Biol 2005; 278: 301-309.
[31] Fischer A, Steidl C, Wagner TU, Lang E, Jakob PM, Friedl P, Knobeloch KP and Gessler M. Combined loss of Hey1 and HeyL causes congenital heart defects because of impaired epithelial to mesenchymal transition. Circ Res 2007; 100: 856-863.
[32] Sakata Y, Kamei CN, Nakagami H, Bronson R, Liao JK and Chin MT. Ventricular septal defect and cardiomyopathy in mice lacking the transcription factor CHF1/Hey2. Proc Natl Acad Sci U S A 2002; 99: 16197-16202.
[33] Tanaka M, Setoguchi T, Hirotsu M, Gao H, Sasaki H, Matsunoshita Y and Komiya S. Inhibition of Notch pathway prevents osteosarcoma growth by cell cycle regulation. Br J Cancer 2009; 100: 1957-1965.
[34] Tradonsky A, Rubin T, Beck R, Ring B, Seitz R and Mair S. A search for reliable molecular markers of prognosis in prostate cancer: a study of 240 cases. Am J Clin Pathol 2012; 137: 918-930.
[35] Wu DC, Zhang MF, Su SG, Fang HY, Wang XH, He D, Xie YY and Liu XH. HEY2, a target of miR-137, indicates poor outcomes and promotes cell proliferation and migration in hepatocellular carcinoma. Oncotarget 2016; 7: 38052-38063.
[36] Cavard C, Audebourg A, Letourneur F, Audard V, Beuvon F, Cagnard N, Radenen B, Varlet P, Vacher-Lavenu MC, Perret C and Terris B. Gene expression profiling provides insights into the pathways involved in solid pseudopapillary neoplasm of the pancreas. J Pathol 2009; 218: 201-209.
[37] Ko BS, Chang TC, Hsu C, Chen YC, Shen TL, Chen SC, Wang J, Wu KK, Jan YJ and Liou JY. Overexpression of 14-3-3epsilon predicts tumour metastasis and poor survival in hepatocellular carcinoma. Histopathology 2011; 58: 705-711.
[38] Barnes DM, Harris WH, Smith P, Millis RR and Rubens RD. Immunohistochemical determination of oestrogen receptor: comparison of different methods of assessment of staining and correlation with clinical outcome of breast cancer patients. Br J Cancer 1996; 74: 1445-1451.
[39] Chang GC, Liu KJ, Hsieh CL, Hu TS, Charoenfuprasert S, Liu HK, Luh KT, Hsu LH, Wu CW, Ting CC, Chen CY, Chen KC, Yang TY, Chou TY, Wang WH, Whang-Peng J and Shih NY. Identification of alpha-enolase as an autoantigen in lung cancer: its overexpression is associated with clinical outcomes. Clin Cancer Res 2006; 12: 5746-5754.
[40] Warner BJ, Blain SW, Seoane J and Massague J. Myc downregulation by transforming growth factor beta required for activation of the p15(Ink4b) G(1) arrest pathway. Mol Cell Biol 1999; 19: 5913-5922.
[41] Claassen GF and Hann SR. A role for transcriptional repression of p21CIP1 by c-Myc in overcoming transforming growth factor beta -induced cell-cycle arrest. Proc Natl Acad Sci U S A 2000; 97: 9498-9503.
[42] Heldin CH, Miyazono K and Ten DP. TGF-beta signalling from cell membrane to nucleus through SMAD proteins. Nature 1997; 390: 465-471.
[43] Luo K. Ski and SnoN: negative regulators of TGF-beta signaling. Curr Opin Genet Dev 2004; 14: 65-70.
[44] Bonnon C and Atanasoski S. c-Ski in health and disease. Cell Tissue Res 2012; 347: 51-64.
[45] Deheuninck J and Luo K. Ski and SnoN, potent negative regulators of TGF-beta signaling. Cell Res 2009; 19: 47-57.
[46] Battaglia S, Benzoubir N, Nobilet S, Charneau P, Samuel D, Zignego AL, Atfi A, Brechot C and Bourgeade MF. Liver cancer-derived hepatitis C virus core proteins shift TGF-beta responses

from tumor suppression to epithelial-mesenchymal transition. PLoS One 2009; 4: e4355.
[47] Qu J, Song M, Xie J, Huang XY, Hu XM, Gan RH, Zhao Y, Lin LS, Chen J, Lin X, Zheng DL and Lu YG. Notch2 signaling contributes to cell growth, invasion, and migration in salivary adenoid cystic carcinoma. Mol Cell Biochem 2016; 411: 135-141.
[48] Yang Z, Guo L, Liu D, Sun L, Chen H, Deng Q, Liu Y, Yu M, Ma Y, Guo N and Shi M. Acquisition of resistance to trastuzumab in gastric cancer cells is associated with activation of IL-6/STAT3/Jagged-1/Notch positive feedback loop. Oncotarget 2015; 6: 5072-5087.
[49] Steidl C, Leimeister C, Klamt B, Maier M, Nanda I, Dixon M, Clarke R, Schmid M and Gessler M. Characterization of the human and mouse HEY1, HEY2, and HEYL genes: cloning, mapping, and mutation screening of a new bHLH gene family. Genomics 2000; 66: 195-203.

Table S1. Primers information

c-Myc	Forward: 5'-GAAAAGGCCCCCAAGGTAGTTA-3'
	Reverse: 5'-TTCTCGTCGTTTCCGCAACAAGTC-3'
β2-MG	Forward: 5'-ATGAGTATGCCTGCCGTGTGAAC-3'
	Reverse: 5'-TGTGGAGCAACCTGCTCAGATAC-3'
p21	Forward: 5'-GGATGAGTTGGGAGGAGGCAG-3'
	Reverse: 5'-CGTTTGGAGTGGTAGAAATCTGTCATG-3'
p15	Forward: 5'-GGGAAAGGATATGTTTATTGACAC-3'
	Reverse: 5'-TGTGCATCCATGGAATGAATATCT-3'

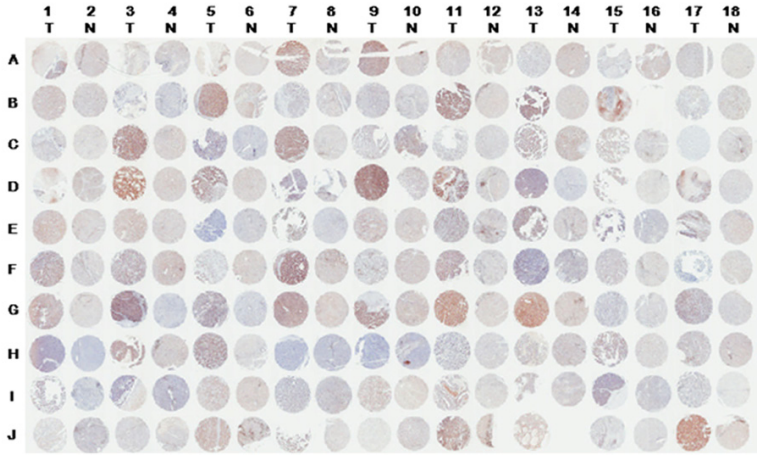

Figure S1. Analysis of HEY2 protein expression in tissues microarray comprising 90 paired HCC tumor tissues (T) and non-cancerous tissues (N).

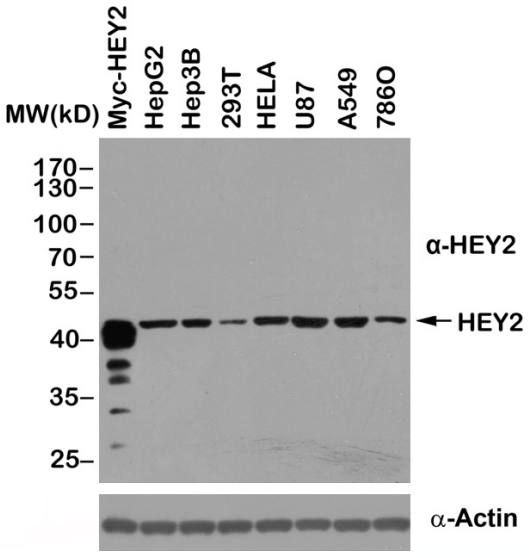

Figure S2. Endogenous HEY2 proteins in HCC cell lines and other tumor type cell lines were examined by western blot using the human HEY2 antibody (NBP1-88629, Novus, 1:300).

Table S2. Number of patients analyzed in tumor HEY2 staining of IHC according to staining intensity and distribution

Distribution	Intensity			
	0 (negative)	1 (weak)	2 (moderate)	3 (strong)
Nucleus				
0 (0%)	9	0	0	0
1 (1-25%)	0	12	7	6
2 (26-50%)	0	4	8	10
3 (51-75%)	0	4	5	18
4 (76-100%)	0	0	0	7
Plasma				
0 (0%)	37	0	0	0
1 (1-25%)	0	6	0	0
2 (26-50%)	0	6	0	0
3 (51-75%)	0	7	1	0
4 (76-100%)	0	17	16	0

Table S3. Correlation of the clinicopathological characteristics with tumor HEY2 expression in nucleus

Variable	HEY2 Expression in nucleus			
	Total, n (%)	Q-score ≤4, n (%)	Q-score >4, n (%)	*P* value
Q-score	90 (100)	50 (56)	40 (44)	
Sex†				
Female	81 (90)	45 (56)	36 (44)	1.000
Male	9 (10)	5 (56)	4 (44)	
Age-yr				
<55	47 (53)	24 (51)	23 (49)	0.423
≥55	42 (47)	25 (60)	17 (40)	
Missing	1			
Tumor size				
<5 cm	35 (39)	20 (57)	15 (43)	0.883
≥5 cm	54 (61)	30 (56)	24 (44)	
Missing	1			
Pathological differentiation				
I-II	57 (63)	31 (54)	26 (46)	0.769
III-IV	33 (37)	19 (58)	14 (42)	
TNM clinical stage				
I-II	40 (49)	20 (50)	20 (50)	0.517
III-IV	42 (51)	24 (57)	18 (43)	
Missing	8			

†Fisher's exact test was used.

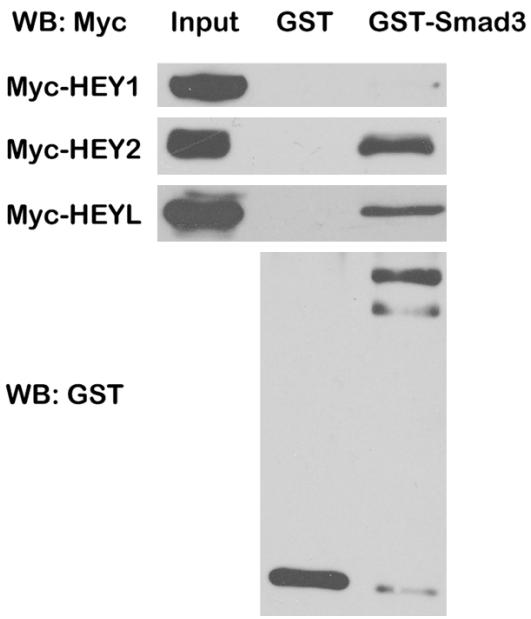

Figure S3. Interaction analysis between HEY family members and Smad3. Bacterially expressed GST and GST-Smad3 fusion proteins were bound to glutathione-Sepharose beads respectively, and then were incubated with Myc-HEY1, Myc-HEY2 and Myc-HEYL proteins. Bound HEY family proteins were detected by western blot with anti-Myc antibody.